1991

A Scanning Tunneling Microscope/Scanning Electron Microscope System for the Fabrication of Nanostructures

Edward E. Ehrichs

Walter Fox Smith
Haverford College, wsmith@haverford.edu

A. L. de Lozanne

A scanning tunneling microscope/scanning electron microscope system for the fabrication of nanostructures

E. E. Ehrichs, W. F. Smith, and A. L. de Lozanne
Department of Physics, The University of Texas, Austin, Texas 78712

(Received 24 July 1990; accepted 4 December 1990)

We have developed an ultrahigh vacuum (UHV) scanning tunneling microscope (STM) designed to work in conjunction with a commercial, high-vacuum scanning electron microscope (SEM). The STM resides in its own UHV subchamber which is housed in the JEOL 820 SEM. We have used the SEM to image the STM tip and its location on the sample. This instrument was built to fabricate and study metallic and contamination resist nanostructures and devices on semiconductor surfaces. To create these structures, we use a technique developed in our lab which uses the STM to dissociate organometallic gases or organic residues on semiconductor surfaces. Our system allows precise alignment of the STM-fabricated structures with underlying macroscopic contact pads. The UHV subchamber, which includes standard UHV sample preparation and analysis equipment, is required to prepare atomically flat and clean samples.

I. INTRODUCTION

The scanning tunneling microscope (STM) is fast becoming an important tool for nanofabrication. It has shown the ability to reproducibly manipulate individual atoms on surfaces[1] making it the highest resolution fabrication technique available. Unfortunately, the STM suffers from a very narrow field of view, making it a difficult instrument to use for device fabrication. We have overcome this problem by designing and building an ultrahigh vacuum (UHV) STM for nanofabrication inside a commercial scanning electron microscope (SEM). STM/SEM systems have been built previously[2,3] but not combining long range x–y motion, UHV, and the ability to handle reactive gases.

In previous work, we have used a conventional high-vacuum STM to deposit metallic features as small as 10 nm.[4] In our technique, organometallic gases are decomposed by applying voltage pulses between the tip and sample, leaving the metal behind on the sample under the tip. We have also used a similar technique to etch 20 nm diameter pits in silicon.[5] However, this previous work was limited by two shortcomings of the apparatus.

The first limitation was the sophistication of the vacuum chamber. Our metallic deposits contained a high percentage of carbon contamination. This may have come from two sources: the carbon contained in the organometallic gases, or residual organic surface contamination. The former can be reduced by using hydrogen as a carrier gas or by using carbon-free precursor gases. Reduction of contamination from the latter source requires a UHV system including sample preparation equipment (annealing and ion milling).

The second serious difficulty with our first system was accurately addressing contact pads on the sample substrate with the STM tip. This would allow 4-probe measurements of STM-fabricated structures, as well as integration of the structures with conventional, lithographically defined devices. Due to the short range of our piezo motion (about 15 μm), accurate sample positioning to within a few microns is required. This was impossible with our old system.

II. THE INSTRUMENT

In order to alleviate these problems, we have built a new STM deposition system. The new system operates under UHV and includes complete sample preparation equipment so that we can atomically clean substrates. The STM is housed in a conventional high-vacuum SEM, so that the precise tip position on the sample can be determined. The system includes long range positioning, allowing the tip to be precisely located over contact pads on the substrate.

The requirements for the chamber are as follows:

(1) It must be easily removable from the SEM so that other experiments can be conducted with the SEM,

(2) it must be a UHV system,

(3) it must isolate the STM from the high vacuum in the SEM chamber to maintain UHV around the STM. It must also prevent precursor gases from reaching the SEM optics.

To achieve the first requirement, the entire STM chamber, sample preparation chamber, and load lock were built onto a cart so that the whole assembly can easily be moved in and out of the SEM chamber (Fig. 1). The cart is built on pneumatic wheels for vibration isolation. The main sample preparation chamber contains a sample load lock, evaporation, rate monitors, an ion gun, sample annealing, and the ability to add low energy electron diffraction or Auger analysis. It is pumped by a 230 ℓ/s ion pump. The sample preparation chamber is connected via a gate valve to the STM chamber. The STM chamber sits inside the SEM providing the required isolation between the two vacuum systems. During STM writing, the gate valve between the sample preparation and STM chambers is closed and vapor deposition precursor gases are added to the STM chamber which is pumped by a turbo molecular pump. For SEM viewing, a small, O-ring sealed shutter on top of the STM chamber is opened, allowing the SEM electron beam to enter through a small aperture. The size of this aperture determines the effectiveness of the differential pumping which isolates the UHV STM chamber from the high vacuum of the SEM. The results shown here were obtained with a 5 mm diameter aperture.

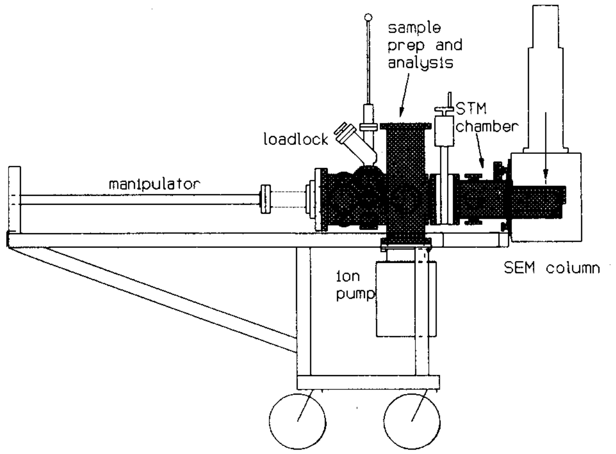

FIG. 1. Diagram showing the sample preparation chamber and STM chamber supported by a cart. The turbo pump (not shown) is attached to the STM chamber through one of the 2.75 in. flanges shown near the gate valve between the STM and sample preparation chambers. Vibration isolation is provided by a 6 in. length of stainless bellows between the turbo pump and the STM chamber.

However, once the correct alignment is determined, we plan to use an insert to reduce the aperture size to 1 mm. We calculate that the pressure in the STM chamber should then be in the low 10^{-9} Torr range, almost 2000 times lower than the pressure in the SEM. Of course, when the SEM is not required, the shutter can be closed, resulting in a substantially lower pressure.

The SEM is a JEOL 820 microscope which was chosen for its reliability, service, and ease of adaptability. We opted for a non-UHV SEM for several reasons. First, the cost of a non-UHV SEM is considerably less than a UHV system. It was necessary for us to build a separate UHV chamber around the STM anyway to contain the precursor gases, so UHV in the SEM was not necessary. Secondly, it is fast and easy to pull our STM chamber out of the SEM (maintaining UHV inside the STM chamber) and put the standard stage back in the SEM for other users. The SEM has a range of magnification from $15\times$ to $300\,000\times$. It also provides a TV rate mode which is necessary for real time positioning of the STM.

For SEM image detection, we opted for a backscattered electron detector in the STM chamber. Certainly a secondary electron detector would provide higher resolution, however, it would have certain disadvantages. First, it would be large, bulky and expensive. Secondly, because a secondary electron detector derives most of its information from low energy electrons (< 50 eV), careful shielding of all high voltages on the STM apparatus would be required to allow these electrons to be collected by the detector.

Although the backscattered electron detector has relatively poor resolution and often poor contrast, it can easily differentiate different atomic number materials (e.g., gold contact pads on silicon) and its resolution is more than adequate for 1 μ contact pads. The detector that we use is a Silicon Detector Corporation #SD100-42-22-231 photodiode with the glass top cut off. The unit costs $50.00 and comes with an on board amplifier. The amplifier has a typical gain bandwidth product of 26 MHz which is sufficient to provide TV rate output. In addition, to attain TV rate, it is necessary to reduce the capacitance of the photodiode by reverse biasing it. We use 18 V of reverse bias. We have set the amplifier to provide a gain of 200 000 V/A and we further amplify the signal outside of the chamber. According to the manufacturer, the amplifier can withstand repeated bakeouts to 150 °C.

The requirements for the STM are as follows:

(1) The STM must be at an angle of 45 deg from horizontal to allow the SEM beam to "see" the tip–sample junction;

(2) the STM must have adequate vibration isolation;

(3) long range x–y motion of the entire STM is required to accurately position the tip–sample junction under the SEM beam;

(4) short range x,y,z motion is necessary for standard STM scanning;

(5) long range z motion of the sample with respect to the tip is required for approaching;

(6) long range x–y positioning of the tip with respect to the sample is required to precisely position the tip over contact pads or an area of interest on the sample;

(7) the ability to change samples and tips *in situ* is required for efficient UHV operation.

The STM resides in its own chamber at 45 deg from horizontal (Fig. 2). It is supported by a stack of stainless steel stages separated by viton spacers, which provide vibration isolation. The stack is supported by an x–y platform driven by two inchworm motors, each with a range of motion of about 1 cm, and a resolution of about 1 nm. This platform allows the STM (tip–sample junction) to be accurately positioned under the SEM beam.

The STM has a concentric tube design.[6] The outer tube supports the tip and provides feedback motion. The inner segmented tube supports the sample and provides x–y and medium range z motion. The inner tube is mounted on an inchworm motor which provides the long range z motion necessary for approach. The two standard UHV inchworm motors and the controlled approach UHV motor (for z approach) are manufactured by Burleigh as are the controller electronics.

The outer piezo tube is mounted on an alumina wafer which slides on three ruby balls. A stick–slip mechanism attached to this wafer (Fig. 3) provides long range x–y motion of the tip with respect to the sample. The stick–slip drivers are two piezo tubes mounted on the wafer at right angles to each other. A 2.5 g stainless steel weight is attached to the free end of each tube. We apply a regular or inverted cycloid waveform[7] to the piezos to provide forward or reverse motion (even uphill at 45 deg). It is necessary for this system to be able to climb uphill because the long range translation must be perpendicular to the tip which resides at an angle of 45 deg from vertical. The resolution of this positioning system is better than 100 nm.

Tips and samples enter the chamber through a small load lock. They can then be transferred to various stages in the sample preparation chamber and finally to the STM by a

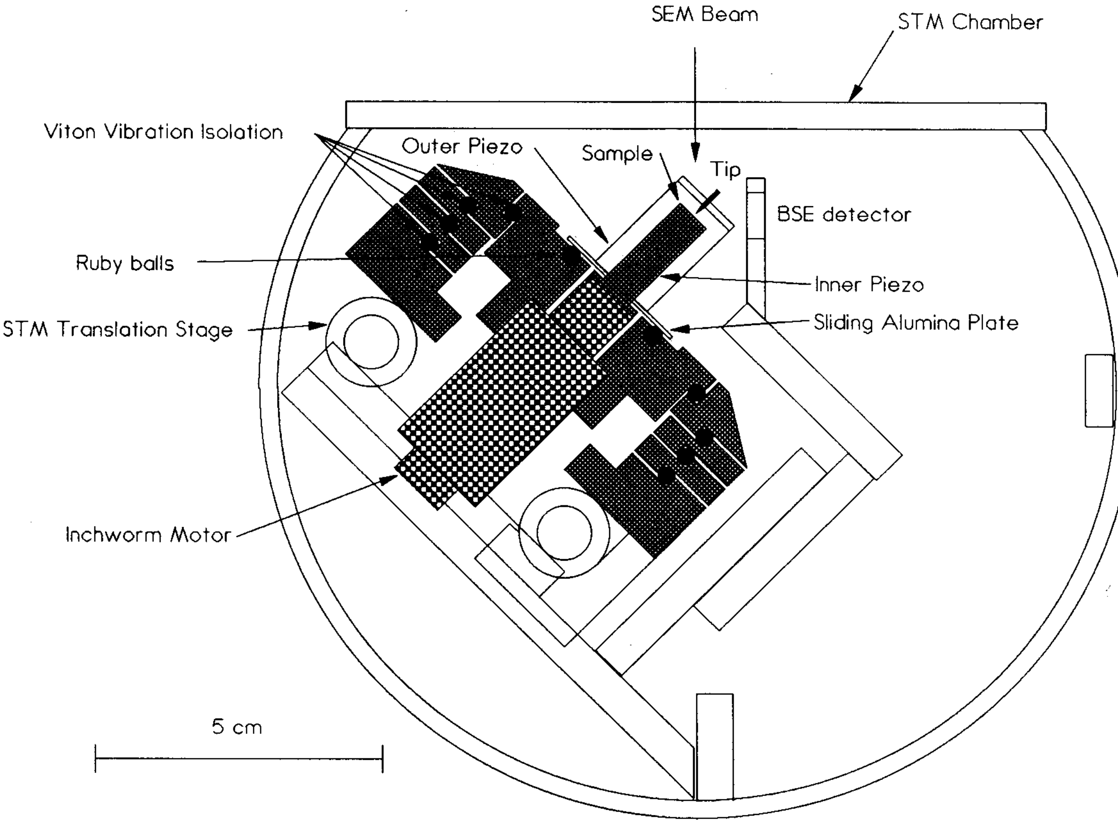

FIG. 2. Diagram of the STM in its UHV chamber.

manipulator arm. Further details on the manipulator design well be given in a future publication.[8]

III. EXPERIMENTAL RESULTS

Figure 4 show successively higher magnification images of the STM tip positioned above a gold and chrome pattern on silicon. The pattern is about 2 mm long by 0.5 mm wide. The large square contact pads on the ends are gold and the lines in between are chrome. In the final image, the tip is over one of the chrome lines.

The image also shows a shadow of the STM tip. Electrons do impinge on the sample surface in the shadow region and generate backscattered electrons. However, these electrons cannot reach the detector, since they are blocked by the tip, and so the shadow is created. This shadow is very useful in judging the distance between the tip and sample. Most of the approach (to within a few microns) can be done very quickly by "eye" moving the sample toward the tip until the tip and its shadow come very close together. The rest of the approach can be done slowly with the computer monitoring the tunneling current. The inchworm positioning system for the STM stage, as well as the stick–slip positioning system for long range motion of the tip relative to the sample, were both thoroughly tested and performed very well. Each of these two positioning systems is controlled by its own joystick. The TV rate SEM image from the backscattered electron detector allows for easy, precise, and rapid positioning.

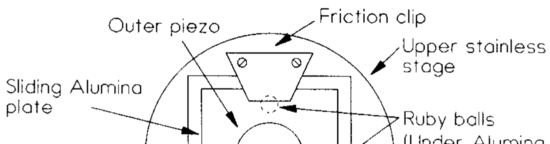

FIG. 3. Diagram of the long range stick–slip positioning system.

Figure 5 shows an STM image taken on the chrome line at the same area as the SEM image. Prior to obtaining this image, we wrote a small dot of "contamination resist" by applying -10 V, 1 μs pulses at 1 kHz for about 1 s to the tip. STM images of this area before writing showed that no such dot existed previously.

We have also tested the STM on highly oriented pyrolitic graphite with a platinum iridium tip to determine its resolution. In this experiment, we obtained atomic resolution, and were able to image the graphite lattice.

IV. CONCLUSIONS

We have designed and built a UHV STM to work inside of a commercial SEM. The system has all of the necessary modes of motion that will be required for fabricating nanodevices at desired locations on sample substrates. We have demonstrated that the SEM and STM work well together. In

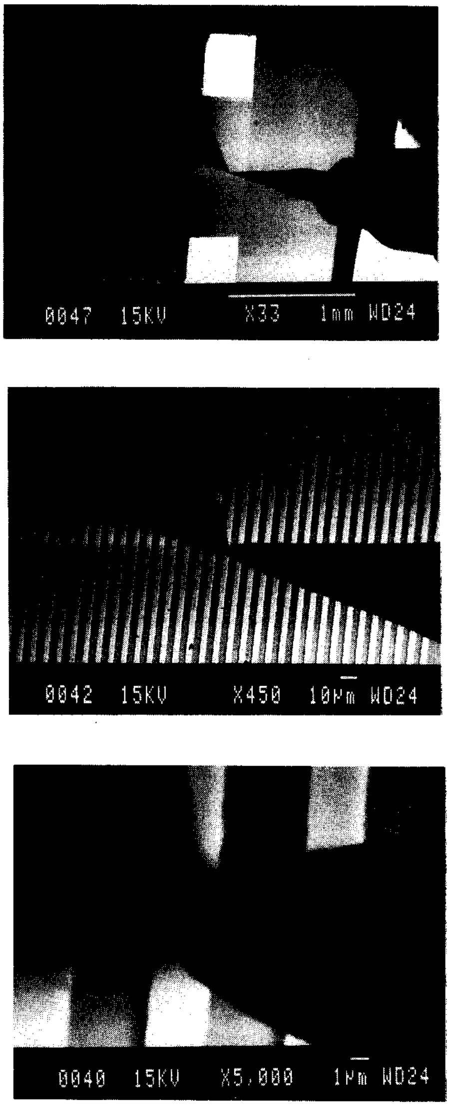

FIG. 4. Three successively higher magnification SEM images of the STM tip positioned above a gold and chrome pattern on silicon.

the near future, we will be testing all of the systems on our chamber and hopefully building some nanodevices. Clearly this instrument will also be very useful for any other STM experiment which requires precise tip positioning or long range motion.

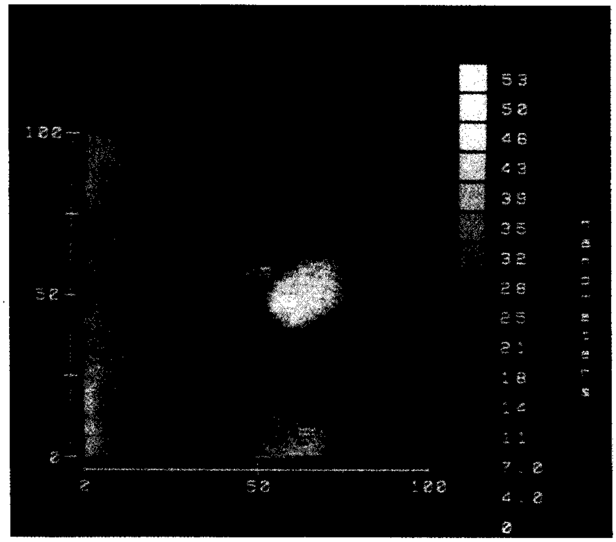

FIG. 5. $100 \times 100\ nm^2$ image of a contamination resist dot written on one of the chrome lines seen in Fig. 4.

ACKNOWLEDGMENTS

This work is supported by the Defense Advanced Research Projects Agency (DARPA), the Welch Foundation, and a Hertz Foundation Fellowship (E. E.).

[1] D. M. Eigler and E. K. Schweizer, Nature **344**, 524 (1990).
[2] Ch. Gerber, G. Binnig, H. Fuchs, O. Marti, and H. Rohrer, Rev. Sci. Instrum. **57**, 221 (1986).
[3] L. Vázquez, A. Bartolomé, R. García, A. Buendía, and A. M. Baró, Rev. Sci. Instrum. **59**, 1286 (1988).
[4] E. E. Ehrichs, S. Yoon, and A. L. de Lozanne, Appl. Phys. Lett. **53**, 2287 (1988).
[5] E. E. Ehrichs and A. L. de Lozanne, J. Vac. Sci. Technol. A **8**, 571 (1990).
[6] C. W. Snyder and A. L. de Lozanne, Rev. Sci. Instrum. **59**, 541 (1988).
[7] Ch. Renner, Ph. Niedermann, A. D. Kent, and Ø. Fischer, Rev. Sci. Instrum. **61**, 965 (1990).
[8] W. F. Smith, E. E. Ehrichs, and A. de Lozanne (in preparation).